

# Crash Compatibility of the Ultralight Steel Auto Body with Cars of the Same Size

**Gustavo A. Aramayo, Srdan Simunovic**

Computer Science and Mathematics Division  
Oak Ridge National Laboratory

**Marcel van Schaik**

Advanced Materials Technology  
American Iron and Steel Institute

Copyright 2000 Society of Automobile Engineers, Inc.

The submitted manuscript has been authored by a contractor of the U.S. Government under contract No. DE-AC05-00OR22725. Accordingly, the U.S. Government retains a nonexclusive, royalty-free license to publish or reproduce the published form of this contribution, or allow others to do so, for U.S. Government purposes.

## ABSTRACT

Computational analysis of vehicle-to-vehicle crashes has been conducted for Ultralight Steel Auto Body (ULSAB) car design. The study involved vehicles of comparable weights and dimensions to assess the compatibility of the ULSAB with existing designs. Deformation and acceleration data for crashed vehicles were analyzed. Vehicle-modeling approaches have strong influence on computational results and the requirements for compatibility of models were identified for future research on vehicle-to-vehicle crash modeling.

## INTRODUCTION

The real challenge of reducing vehicle weight is to meet and exceed safety standards without sacrificing affordability. Ultralight Steel Auto Body (ULSAB), shown in Figure 1, is steel-based concept to achieve such weight reduction. In 1994, thirty-five steel companies formed the global UltraLight Steel Auto Body Consortium to build a body structure that weighed 203 kg, exceeded all structural requirements, and offered a high degree of safety, while maintaining the affordability and 100 percent recyclability of steel. At 203 kg, ULSAB has a body mass that is 25 percent less than average benchmark vehicles and up to 36 percent less than the average N-A mid-size body structure. ULSAB, a \$22 million program, achieved its aggressive targets through the use of advanced technologies and materials combined with innovative design. The body structure comprised only 96 major parts and 158 total parts, compared with more than 200 parts for a typical auto body. High-strength (HS) and ultra-high-strength (UHS) steels account for more than 90 percent of the material. Half the mass comprised tailor-welded blanks (TWBs). Two other elements are the hydroformed side roof

rail and the steel sandwich used for the spare tire tub and dash panel insert.



Figure 1. ULSAB Vehicle

With regards to crash events, the tests and current requirements in Table 1 were taken into consideration.

Crash Event	ULSAB Program	PNGV NHTSA requirements
Frontal	35 mph (+36%)	30 MPH
Frontal Offset	34 mph 50% offset	No
Side	31 mph 90 degree	33.5 mph 63 degree
Rear	35 mph	30 mph
Roll Over	1.5 x curb weight	1.5 x curb weight

Table 1. Crash Simulations Used in ULSAB Design

Crash performance was evaluated by using computer simulations; the simulations indicated that the vehicle would satisfy all the listed safety standards.

The recent initiatives by transportation safety agencies to consider different deformable and offset-barrier crash-test scenarios and technologies together with car-to-car impact evaluations indicate that the safety requirements will become broader and more stringent. Numerous publications, (see for example References 1-4, and references listed therein), have appeared on the subject of crash compatibility. These publications generally address aspects of compatibility in the existing passenger fleet; and therefore, analyze standard design features. The three main factors influencing crash compatibility, namely curb mass, body stiffness and body geometry, are different for the ULSAB design relative to conventional car design. The need for car-to-car crash compatibility analysis is therefore justified and was the objective of the research presented in this paper. This research takes advantage of ongoing automotive-related activities at the Oak Ridge National Laboratory (ORNL), the National Highway Traffic Safety Administration (NHTSA), and NHTSA contractors aimed at developing vehicle models that are representative of the vehicles in the U.S. car and truck fleet.

Characteristic crash-response parameters associated with crash-energy management in the frontal car-to-car impact simulations are discussed. The research work reported in the paper was conducted in 1998.

## METHODOLOGY

The crash compatibility of the ULSAB with cars of similar weight and geometric characteristics is assessed using the results of computer numerical simulation of the crash scenario that depicts the frontal collision with full engagement (no offset) of two cars, each with a forward velocity of 13.4 m/s (35 mph). One of the cars is the ULSAB car. The other car is representative of an existing four-door passenger vehicle in the current U.S. fleet.

The uncoupled finite-element (FE) models of the vehicles representing the U.S. fleet have been developed for the NHTSA by different institutions. The vehicle models used in this study (Ford Taurus, Chevrolet Lumina, and the Dodge Intrepid) were developed by EASi Engineering, Inc. References 5 and 6 describe the model developments for the Ford Taurus; Reference 7 describes the development of the FE models for the Chevrolet Lumina and the Dodge Intrepid. Porsche Engineering Services, Inc., developed the FE model of the ULSAB [8].

The results of the numerical analysis provide parameters that are used for comparison of the crash responses of the vehicles involved. Crash compatibility is evaluated using the deformation of the frontal area (crush-zone, CZ) of the cars and the integrity of the occupant compartment (OC). The deformation of CZ is quantified by the dimensional change measured in the longitudinal axis of the cars between a point on the bumper and a point on the firewall. The reduction in the distance between points at the base of the B-pillar of ULSAB relative to the same point on the other car reflects the severity of the frontal collision. Calculated acceleration traces and their average values can also be used as indicators of the severity of the

collision. Finally, the forces in the ULSAB's frontal main load-carrying members in the car-to-car crashes are compared to the forces from the NHTSA New Car Assessment Program (NCAP) test that was one of the ULSAB design requirements (see Table 1).

The computer simulations of the car-to-car collisions were performed using the LS-DYNA computer program [9]. The assembly of the crash scenarios uncoupled car was done with program LS\_INGRID. The numerical work was performed on a multiprocessor SGI-Origin 2000 and IBM RS6000 SP2 supercomputers.

## FINITE-ELEMENT MODELS

Numerical analyses were performed for the crash scenarios that depicted the following frontal-collision events:

- ULSAB-1992 Ford Taurus
- ULSAB-1995 Chevrolet Lumina
- ULSAB-1994 Dodge Intrepid

These vehicles are four-door, front-end-driven production models. All major structural components, including the body-in-white, are made of steel. Ford Taurus, Chevy Lumina, and Dodge Intrepid are classified as mid-size passenger cars, and are typical of the existent passenger cars in the U.S. fleet. The ULSAB car is a concept vehicle; this is a four-door, front-end driven, transverse-mounted-engine/transmission vehicle with relatively low structural weight. Geometrically, both the concept and target vehicles are similar in bumper heights and general body dimensions.

An overview of the uncoupled vehicle FE models is shown in Table 2. The FE models of the target vehicles were obtained courtesy of NHTSA [10].

<i>Vehicle</i>	<i>Node</i>	<i>Solid</i>	<i>Beam</i>	<i>Shell</i>
ULSAB	174294	0	934	177326
Taurus	26737	340	140	27873
Lumina	100769	3168	106	92960
Intrepid	90191	3732	118	82728

Table 2. FE Model Statistics of Vehicles used in Analysis

The level of complexity in the models has progressed in time as computational resources were made available and as refinements in analysis tools were implemented. The oldest model is the Ford Taurus, developed in 1993. The later models show significant increases in the number of elements as well as other refinements offered by the analysis software. Reference 11 can be consulted for in-depth background information on vehicle crashworthiness modeling and design.

The uncoupled models have been extensively verified and validated in several crash scenarios [7], one of which is the frontal collision with a flat rigid barrier (NCAP test).

Validation and verification of each model were also conducted in house before the coupled model was generated. No changes have been made to the uncoupled models before the assembly of the full model used in the analysis. The total crash mass of the car models used in this project is given in Table 3.

<i>Vehicle</i>	<i>Total Crash Mass</i>
ULSAB	1612
Taurus	1563
Lumina	1754
Intrepid	1682

Table 3. Calculated Vehicle Mass (kg)

The total crash mass of the vehicles also depends on the level of accessories, occupants, and luggage included. A detailed description of the additional weight for each of the vehicle was not available and may have caused the disparity between the real masses. However, the weights of the U.S. fleet vehicles were similar to the NCAP test weights reported in the NHTSA crash test database.

With regards to the detail of the FE models, some vehicle components were not included in the models. The ULSAB model did not include the engine lid, trunk lid, or glass panels in the front and rear doors; Chevy Lumina and Dodge Intrepid models did not have the rear and front doors. However, these components were included in the total crash mass of the vehicles.

### 1-Material Data

The uncoupled FE models for all the vehicles in the study use material type 24 of the LS-DYNA [9] repertoire; no strain rate dependency is used, and the stress-strain relationship is given in tabular form. Yield stresses and plots of stress-strain curves for these materials, for the structural components found in the frontal crush zone are given in the paragraphs that follow.

The ULSAB materials range in yield stress values from 140 to 800 MPa (Figure 2).

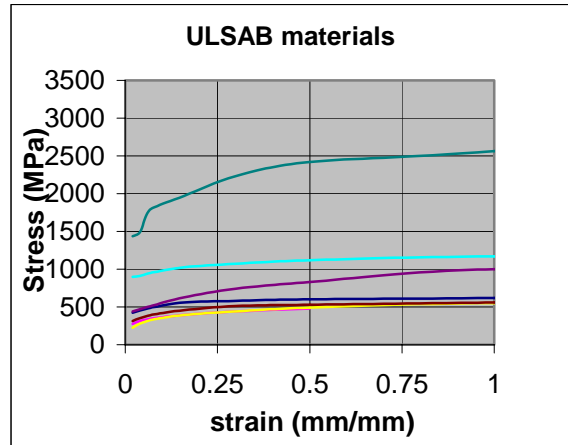


Figure 2. Material Data for ULSAB

The Taurus material yield stress is 215 MPa (Figure 3).

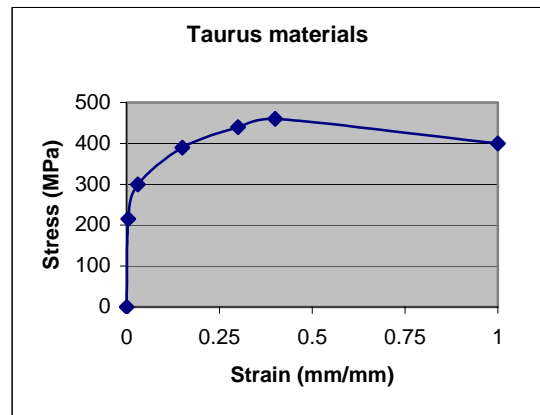


Figure 3. Materials for Taurus

The Lumina material yield stress is 210 MPa (Figure 4).

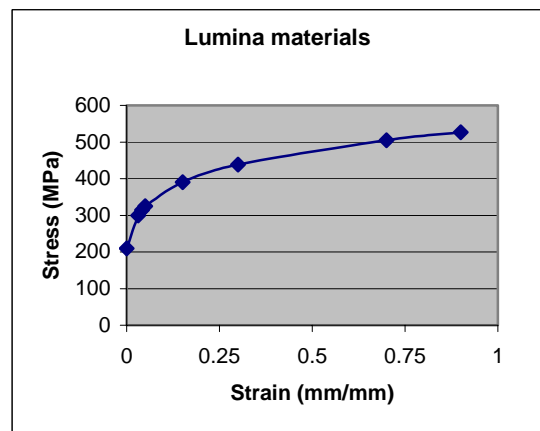


Figure 4. Materials for Lumina

The Intrepid materials range in yield stress values is from 210 to 273 MPa (Figure 5).

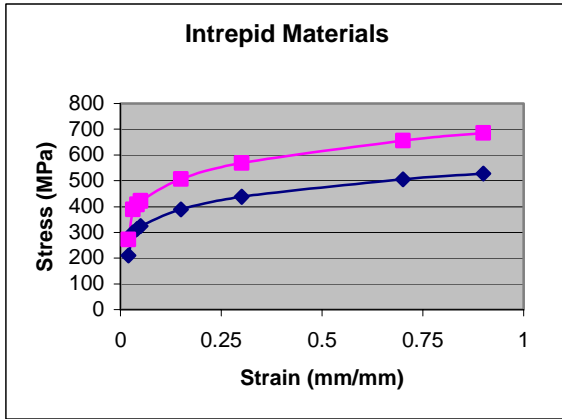


Figure 5. Materials for Intrepid

The data used in the above figures have been directly extracted from the uncoupled vehicle models.

## 2-Finite-Element Formulations

Shell elements in the FE models are based on the Belytschko-Tsay formulation. For consistency in the analysis, the most computationally conservative control parameters from the uncoupled models were used. Typical 10x10 mm aspect ratio is found in most of the shell elements. The Ford Taurus model has a larger shell aspect ratio simply because of the vintage of software and hardware available at the time the model was developed. Most of the beam elements used in the models are based on the Belytschko-Schwer formulation. The model of Chevy Lumina uses some Hughes-Liu beams.

In general, a unique contact formulation has been used (LS-DYNA3D type 13, defining a volume that includes the entire two cars). The coupled FE model also prescribes a rigid reference base defined using a "stonewall" that is not shown graphically.

## NUMERICAL SIMULATIONS

Results of the numerical simulation of each of the three cases considered in the study are briefly discussed in the sections that follow.

### ULSAB-Taurus Collision

This section discusses the results of the simulation of the frontal collision of ULSAB and the 1992 Ford Taurus (Figure 6). The ULSAB model is slightly heavier than the Taurus model (1612 kg vs. 1563 kg). The physical dimensions of both cars are comparable.



Figure 6. Taurus-ULSAB Collision Model

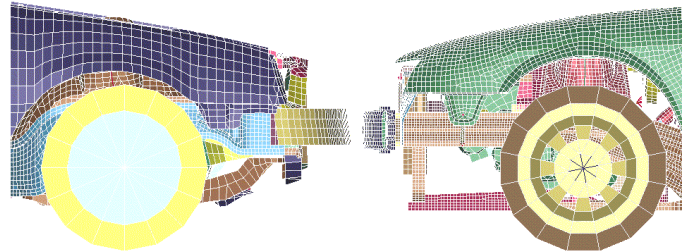


Figure 7. Initial Configuration- Taurus-ULSAB

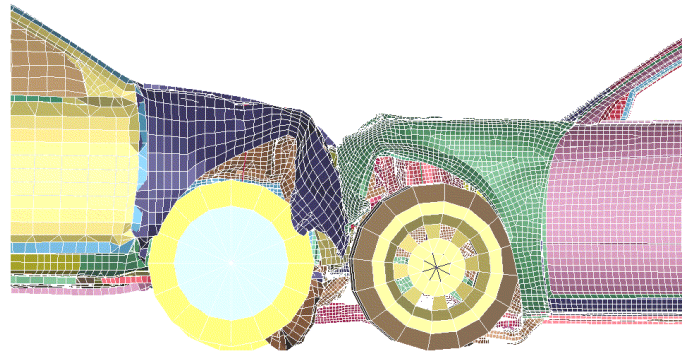


Figure 8. End of Simulation- Taurus-ULSAB

Figures 7 and 8 show the side view of the initial ( $T_0$ ) and final simulation time ( $T_{end}$ ) configurations of the frontal collision. Head-down view is shown in Figures 9 and 10.

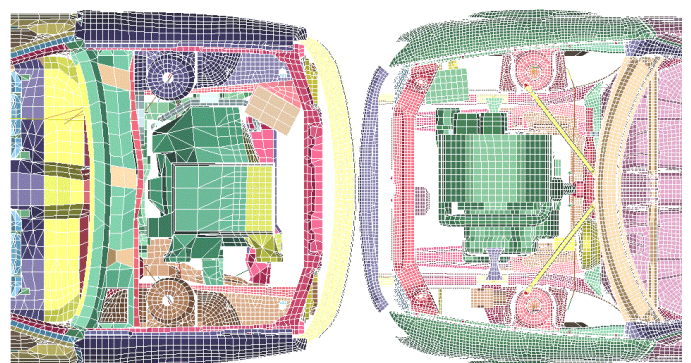


Figure 9. Overhead View, Initial Configuration



Figure 10. Overhead View, Final Configuration

The frontal region of Taurus progressively collapses during the first 20 ms from contact initiation. Subsequently, the engine cradle (sub-frame) of the Taurus undergoes large bending so that, after 35 ms from contact initiation, the engines of both cars make contact. Displacement of the engines is the driving mechanism that generates the deformation to the engine sub-frame. The engine remains attached to the sub-frame through the collision.

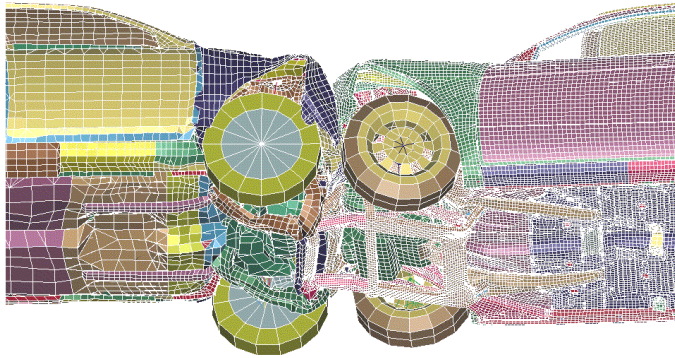


Figure 11. Deformed Configuration of Frame

The deformation in the undercarriage of the vehicles is shown in Figure 11 at a time when the kinetic energy is at a minimum ( $T_{v=0}$ ). A large deformation in the occupant compartment floor of the Taurus car that is associated with the loads imposed in this region by the engine cradle rear support point. Limited motion of the engine of ULSAB relative to its engine attachment points can be observed.

The reduction in lengths of the crush zones measured from the front of the bumper to a point in the firewall at time  $T_{v=0}$  is shown in Table 4.

Vehicle	X reduction (mm)	X reduction (% of initial)
ULSAB	566	48
Taurus	634	58

Table 4. Reduction of Length in Crush Zone

The longitudinal component of the change in length between points at the base of the B-pillar in the driver side

of the ULSAB and the passenger side of the Taurus model, at time  $T_{v=0}$  is 1257 mm. The door frame of the Taurus undergoes deformation due to the bending of the upper rail of the doorframe. The reduction in length of the passenger floor measured from the firewall to the front of the driver seat is 10 mm and 166 mm for the ULSAB and Ford Taurus models, respectively.

The average acceleration values along the longitudinal car axes at two locations, the low B-pillar at the rocker panel elevation and in the occupant floor just below the driver seat, for each of the vehicles are given in Table 5. Average accelerations have been calculated in time interval between  $T_0$  and  $T_{v=0}$ .

Vehicle	Base B-pillar	Floor below driver seat
ULSAB	18	16
Taurus	22	18

Table 5. Accelerations (G's) at Selected Locations

Figures 12 and 13 show the time history of accelerations at the selected locations.

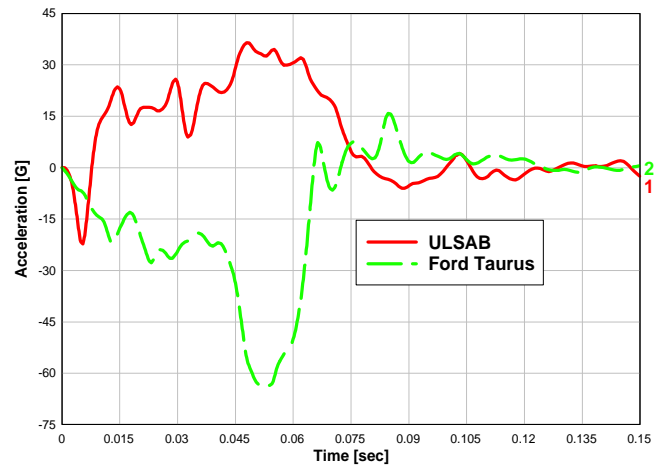


Figure 12. X-Acceleration at Base of B-Pillar

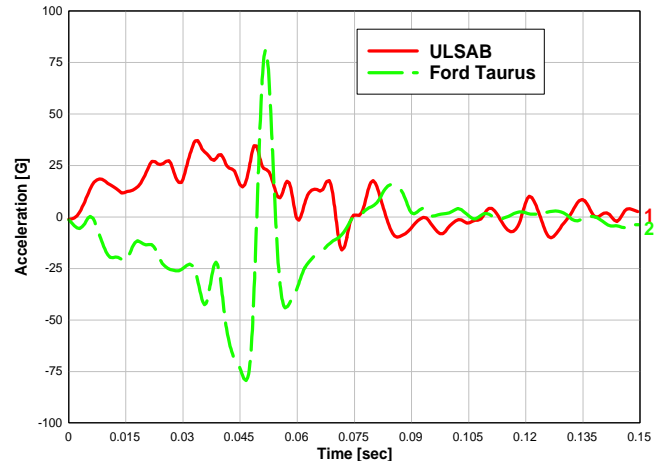


Figure 13. X-Acceleration at Driver's Side Floor

The forces carried out by the frontal structural crash zone components are displayed in Figure 14. The cross sections used for force calculations were placed in the rear base of the rails to estimate the forces transferred to the OC. Lower rail has sustained level of 70 kN and peak force of 100 kN. The sub-frame has a higher peak than the upper rail.

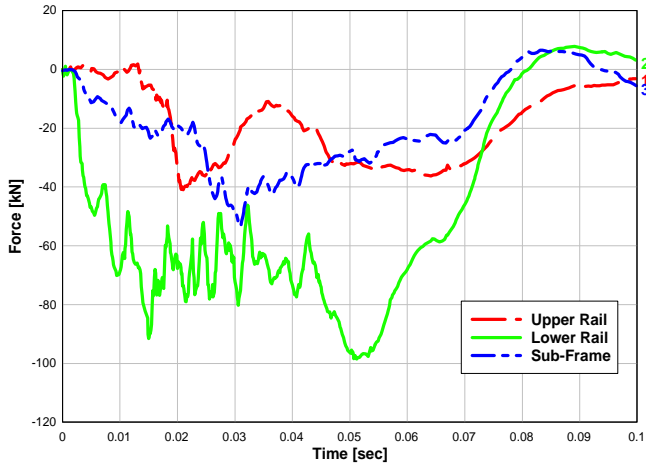


Figure 14. Front Rail Forces in ULSAB

ULSAB-Chevrolet Lumina Collision



Figure 15. Lumina-ULSAB Collision Model

This section discusses the results of the simulation of the frontal collision of ULSAB and the 1995 Chevrolet Lumina models (Figure 15). The Lumina model is about 9% heavier than the ULSAB (1754 kg vs. 1612 kg). The physical dimensions of both cars are comparable.

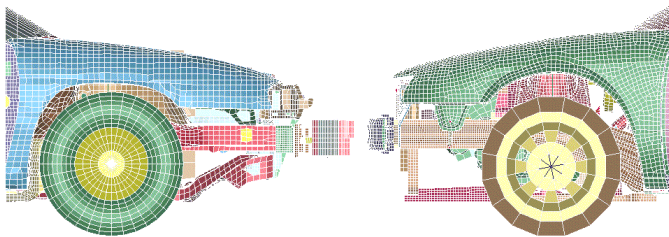


Figure 16. Initial Configuration, Lumina-ULSAB

The side view of the two vehicles at the beginning of the simulation given in Figure 16 shows good alignment of the centroidal axis of the rail sections near the bumper attachment points.

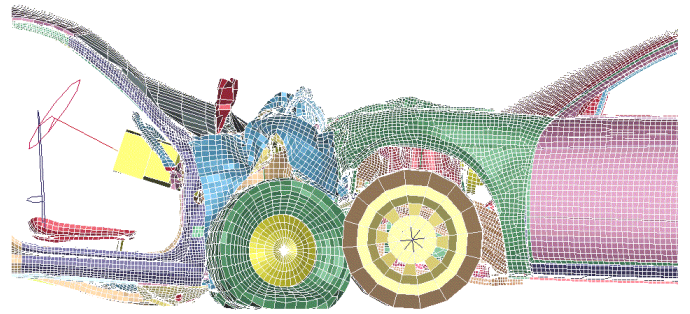


Figure 17. End of Simulation, Lumina-ULSAB

The configuration at the end of the simulation of the vehicles is shown in Figure 17, and Figures 18 and 19 show the heads-down view of the initial and final simulation configuration of this collision.

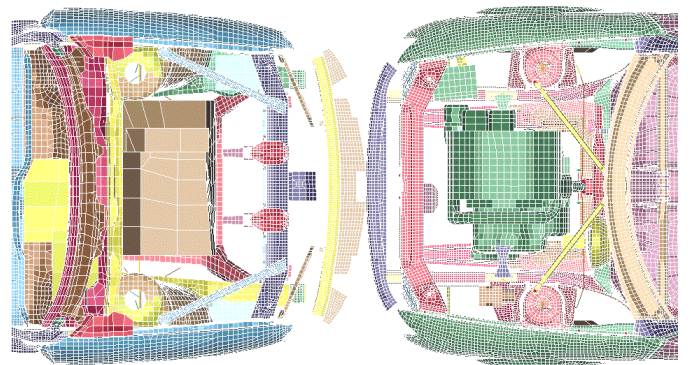


Figure 18. Overhead View, Initial Configuration

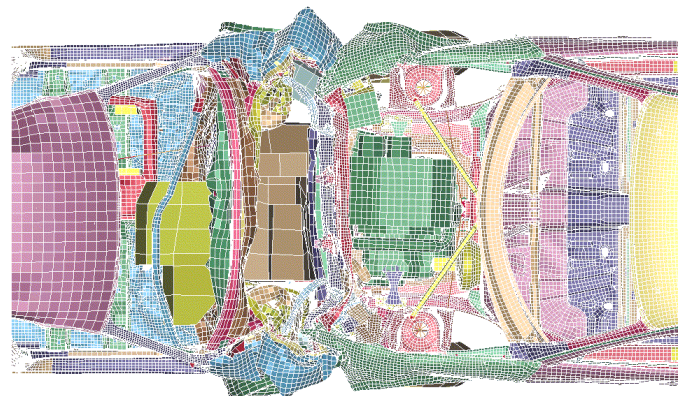


Figure 19. Overhead View, Final Configuration

Deformation of the Lumina's front structure is considerably larger than that of the ULSAB. It can be attributed to the collapse of the lower rail and the lower frame assembly (engine cradle) that supports the engine, drive train, and front suspension. During the frontal collision the sub-frame develops a plastic hinge near the engine support points. The engine remains attached to the engine cradle and

causes the supports of the engine cradle that are attached to the floor to undergo large displacement. Large free space between the engine and radiator assembly in the Chevy Lumina model allows the ULSAB to translate into the Lumina's crush zone before significant loads in the forward assembly are developed. The engines of both cars make contact 37 ms from initiation of impact. The reduction in length of the section between the firewall and the front bumper along the center axis of the vehicles is given in Table 6.

Vehicle	X reduction (mm)	X reduction (% of initial)
ULSAB	493	42
Lumina	882	71

Table 6. Reduction in Length in Crush Zone

The overall longitudinal component of the change in length between points at the base of the B-pillars in the driver side of the ULSAB and the passenger side of the Lumina model is 1622 mm. The dimensional (reduction) change in the floor area just in front of the driver seat and behind the firewall for the ULSAB is 5 mm. The corresponding change in dimension for the Lumina is 196 mm.

The filtered acceleration data is shown in Figures 20 and 21. The average values between  $T_0$  and  $T_{v=0}$  are reported in Table 7.

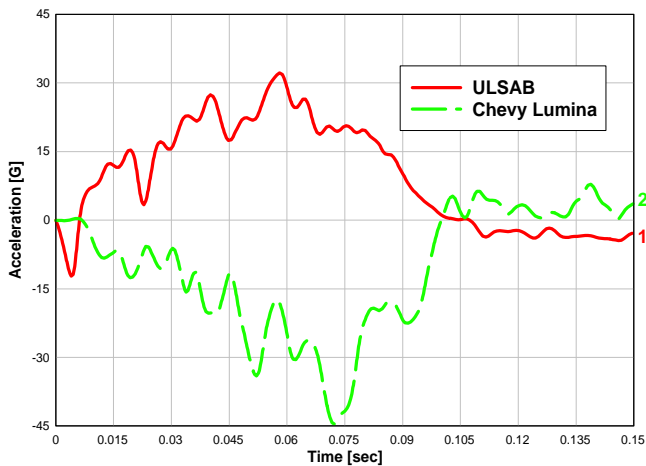


Figure 20. X-Acceleration, Base of B-Pillar

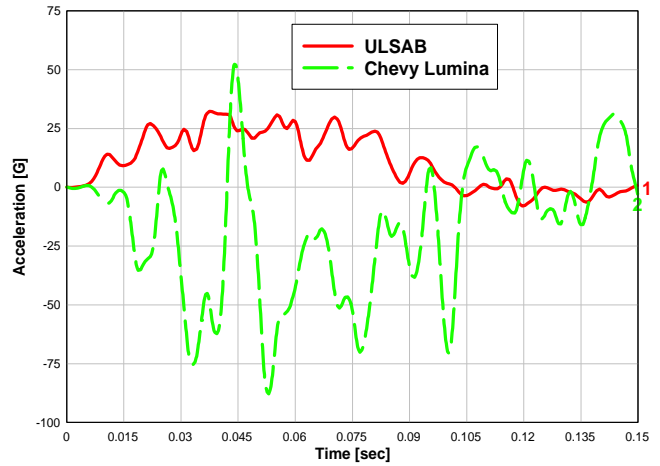


Figure 21. X-Acceleration, Driver's Side Floor

Vehicle	Base B-pillar	Floor below driver seat
ULSAB	17	19
Lumina	18	28*

\*High frequency component data, unreliable.

Table 7. Average Accelerations (G's) at Selected Locations

The traces of force in the forward assembly of the ULSAB vehicle are shown in Figure 22. The duration of the sustained force in the lower rail is 20 ms longer compared to the Taurus - ULSAB collision simulation.

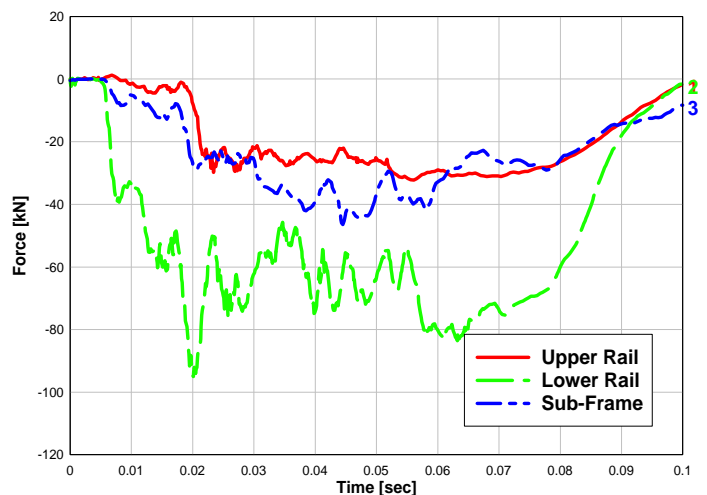


Figure 22. Front Rail Forces in ULSAB

## ULSAB-Dodge Intrepid Collision



Figure 23. Dodge Intrepid-ULSAB Collision Model

The frontal collision of the ULSAB and the Dodge Intrepid is considered in this section (Figure 23). The Intrepid is 4% heavier than ULSAB (1682 kg vs 1612 Kg). Figure 24 shows the bumpers mismatch (40 mm). The corresponding configuration at the end of the simulation is shown in Figure 25.

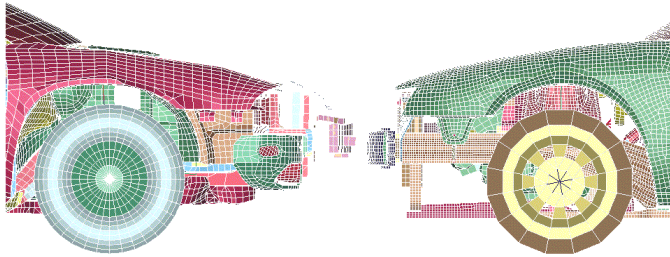


Figure 24. Initial Configuration, Dodge Intrepid-ULSAB

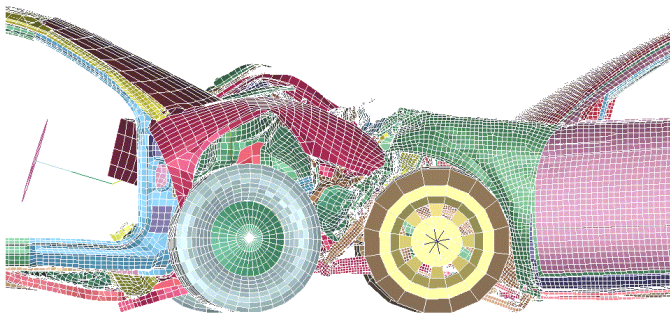


Figure 25. End of Simulation, Intrepid-ULSAB

Both vehicle models experience large deformation of the corresponding crush zones. In the ULSAB this deformation is due to the progressive collapse of the lower rail. A plastic hinge-like mechanism occurs at the engine mount location and rear attachments of the sub-frame. The deformation in the crush zone of the Intrepid is limited by the forward location of the engine. The engines make contact at 38 ms from initiation of impact.

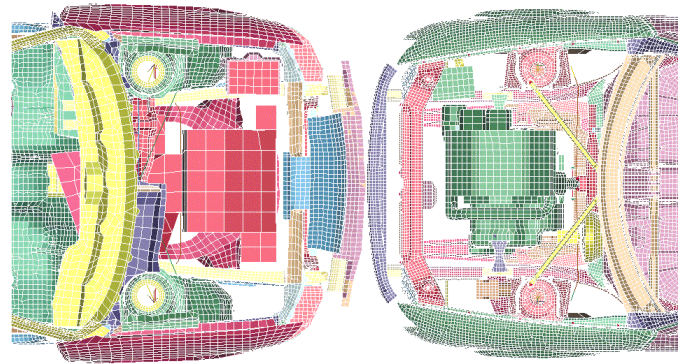


Figure 26. Overhead View, Initial Configuration

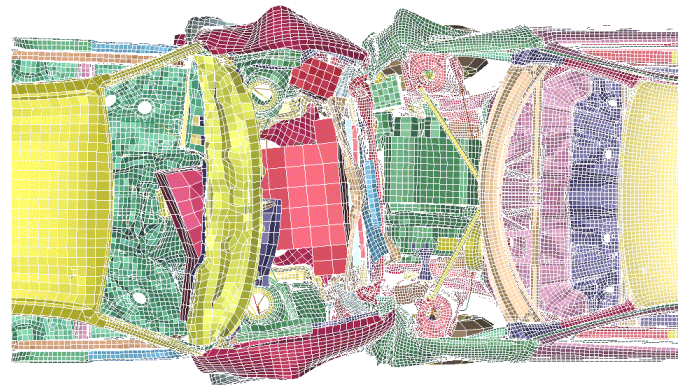


Figure 27. Overhead View, Final Configuration

Heads-down views at the beginning and end of the collision simulation are given in Figures 26 and 27. The motion of the engines can be assessed using the strut towers as reference points. In both cars this motion is attributed to the deformation of the sub-frames that support the engines. Engine supports are not allowed to break-off in the models. Consequently, the engines impart large deformations on the sub-frames and lower rails and control their collapse mechanisms. Figures 28 and 29 illustrate the extent of deformation in the sub-frames.

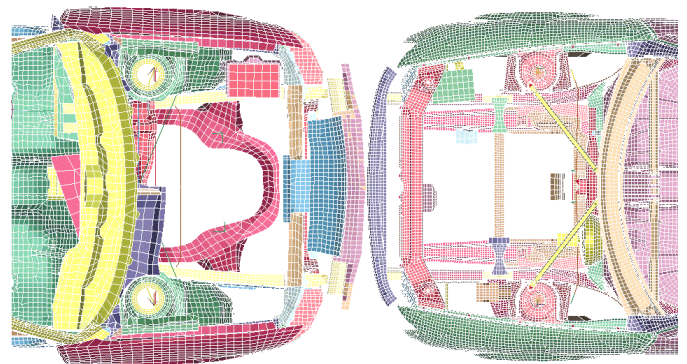


Figure 28. Sub-Frame Initial Configuration



Figure 29. Sub-Frame Final Configuration

The reduction in length of the crush zones is shown in Table 8. The change in length between the bases of the B-pillars in both cars is 1526 mm.

Vehicle	X reduction (mm)	X reduction (% of initial)
ULSAB	662	56
Intrepid	721	58

Table 8. Reduction in Length in Crush Zone

The floor intrusion in the driver-side floor is 10 mm for the ULSAB and 230 mm for the Dodge Intrepid model. Traces of nodal accelerations at the base of the B-pillar and at the floor below the driver seat are given in Figures 30 and 31. The average values are given in Table 9.

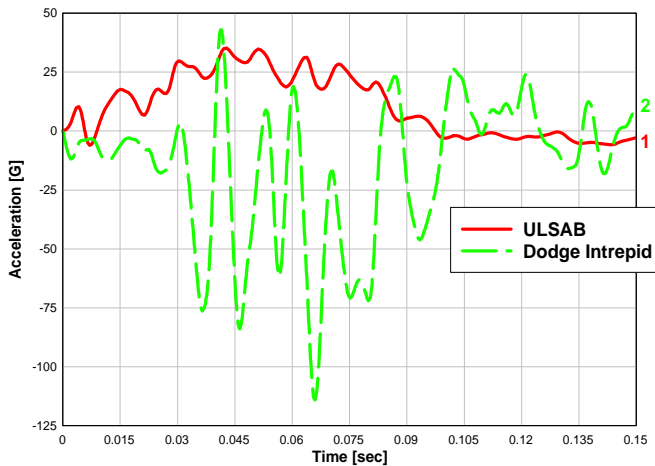


Figure 30. X-Acceleration, Base of B-Pillar

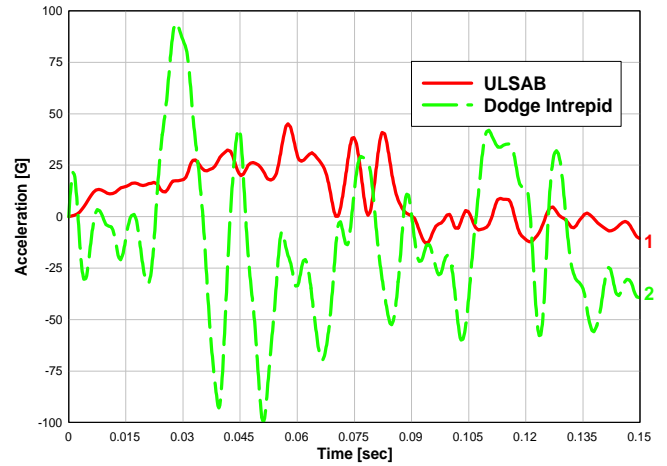


Figure 31. X-Acceleration, Driver's Side Floor

Vehicle	Base B-pillar	Floor below driver seat
ULSAB	20	20
Intrepid	27	9*

High frequency component data, unreliable.

Table 9. Accelerations (G's) at Selected Locations

The forces in the longitudinal main load-carrying members in the ULSAB car are given in Figure 32. The bumpers mismatch does not seem to have a significant influence on the overall force levels in the ULSAB model.

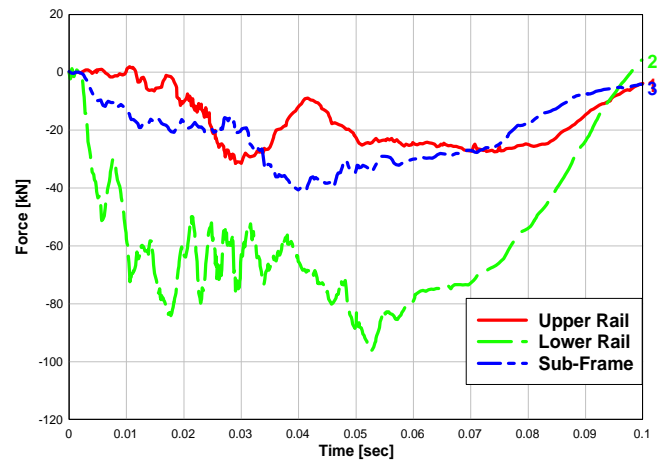


Figure 32. Front Rail Forces ULSAB

## DISCUSSION OF RESULTS

The results of numerical simulations of the front-end collision of the ULSAB concept car with models of passenger cars in the U.S. fleet have been presented in the previous sections. The study has been undertaken to assess the crash compatibility of the 'concept' car with cars with similar weight and geometric characteristics. A

companion goal of the study was to investigate the feasibility of computational simulations for crash compatibility analysis using car models that employ different structural designs and modeling approaches.

Crash compatibility has been addressed from two points of view: a structural view in which the integrity of the ULSAB is compared with the integrity of the companion car, and a safety consideration that addresses the deceleration and integrity of the OC. The structural response of ULSAB in a frontal collision is assessed in terms of the reduction in the axial length of the crash-absorbing structure in front of the OC. Figure 33 shows the normalized reduction in length of the CZ for the ULSAB and the companion vehicle model for each of the “crash events” analyzed where the “event number” denotes ULSAB collision with the Ford Taurus, Chevy Lumina and Dodge Intrepid, respectively.

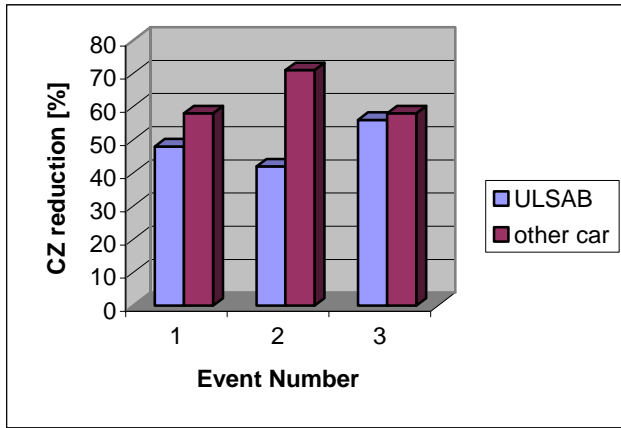


Figure 33. Comparison of Crush Zone Lengths

The label “other car” denotes the matching car model in the corresponding collision event (Ford Taurus, Chevy Lumina, and Dodge Intrepid). Comparisons of the average acceleration levels at two locations in ULSAB that are associated with the car-to-car collision are shown in Figures 34 and 35.

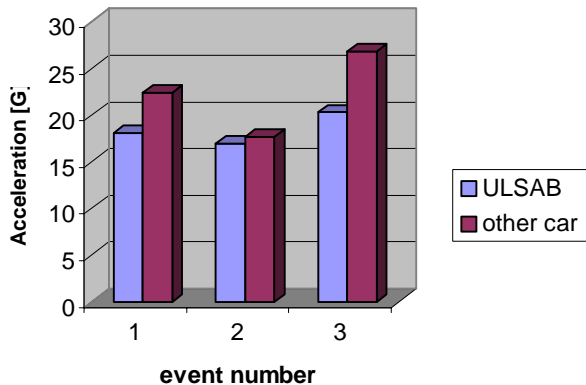


Figure 34. Average Acceleration at Base of B-Pillar

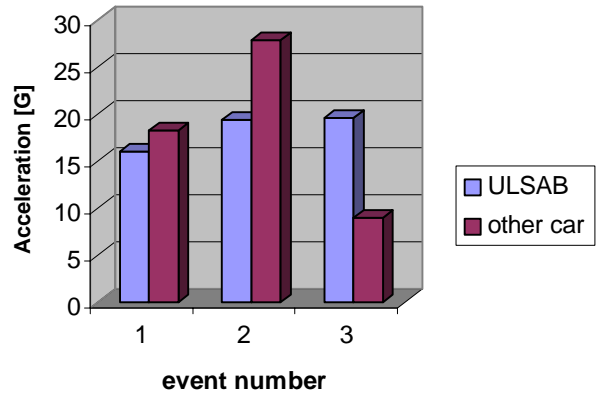


Figure 35. Average Acceleration in Occupant Floor

For the ULSAB model, the acceleration levels at the base of the B-pillar are proportional to the reduction in length of the CZ. The accelerations in the floor area below the driver’s seat exhibit markedly fewer oscillations in the ULSAB model than for the companion car model and, therefore, the two cannot be reliably compared. The floor accelerations in ULSAB depend largely on the deformation of the sub-frame and its attachment to the floor. Typical average acceleration values for vehicle-to-vehicle full frontal crash tests as reported in Reference 12 are between 8 and 20 G’s. The calculated values in this analysis fall close to this range.

Table 10 shows the reductions in length (floor intrusion) in front of the driver’s sides in each of the crash events. In general, the floor intrusion in the ULSAB is smaller than the intrusion on the companion car model. This is attributed to the larger stiffness of the CZ in the ULSAB relative to the companion car. The stiffness of the rail that supports the engine, the engine mount, and the attachment of the engine cradle to the floor contribute to the deformation of the occupant floor.

Crash Event.	ULSAB	Other Car
ULSAB-Taurus	-10	-166
ULSAB-Lumina	-5	-196
ULSAB-Intrepid	-10	-230

Table 10. Floor Intrusion

Floor intrusion in the ULSAB model can be linked to the kinematics of the engine and to the relative stiffness of its supports. Table 11 shows the reduction in distance between the bases of the B-pillars of the two cars involved in the collision (driver side of ULSAB - passenger side of the companion car), and the sum of the reduction in CZ of both cars for each collision.

Crash Event	B-Pillar to B-Pillar	Sum of CZ
ULSAB-Taurus	1257	1200
ULSAB-Lumina	1622	1375
ULSAB-Intrepid	1526	1383

Table 11. Dimensional Change Between Points at Base of Vehicle B-Pillar Points and Summation of CZ

The difference in these two columns is due to the contribution of rigid body motions. The summation of reductions in CZ's seems to offer a better indication of crash performance because it does not include the rigid body movements. Time traces of forces for the bases of the upper rail, lower rail, and engine cradle of the ULSAB CZ have been shown in the Figures 14, 22 and 32. The peak load value for all the cases considered is 100 kN. From the crash-compatibility aspect, magnitude and character of forces in these structural members offer good measures for the ULSAB crash compatibility. Figure 36 presents the traces of load in the ULSAB main rails for the NHTSA NCAP test. The character and the magnitude of force-time curves are very similar to the rail forces associated with the simulated car-to-car collisions. The main differences are the crash duration, and the peaks in the upper rail and sub frame. For NCAP, the upper rail has pronounced high peak of 55 kN compared to more gradual and sustained response for the car-to-car collisions where the maximum value is 40kN.

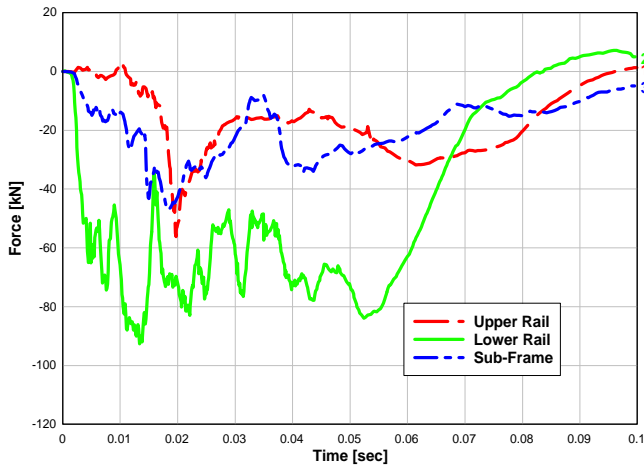


Figure 36. Rail Forces in ULSAB, NCAP test

## CONCLUSIONS

Results of the project conducted to assess the crash compatibility of ULSAB with cars of similar geometric characteristics have been presented and discussed in this paper. This is a computational study that had the objective of quantifying the crash compatibility of ULSAB relative to cars with similar geometric and inertia characteristics. Experimental verification has not been conducted and, as such, the study is confined to the realm of computational modeling.

The following conclusions can be drawn from the results of the study:

- In general, the design of ULSAB is compatible with the design of existing cars with similar inertia and geometric characteristics.
- The structural-performance characteristics of the vehicles involved in a car-to-car collision when one of the cars is the ULSAB are governed by the stiffness and geometry of the CZ in the vehicles.
- The effects of mass, being traditionally one of the most important parameters used to assess compatibility, could not be evaluated because of the similar mass of the vehicle models used in the analysis. Within the constraints of the current analysis it appears that, for the ULSAB, the effects of stiffness dominate the compatibility aspects for collisions with similar vehicles.

The study identified several areas that should be carefully considered to computationally simulate crash-compatibility:

- There is a need for establishment of general guidelines for model development if models from different sources are to be used in compatibility analysis. Models used in this study employed different approaches for materials modeling, element distribution, and connection between vehicle components.
- Modeling of the engine kinematics and attachments needs to be improved and verified experimentally. The current engine mount models seem to be too simplistic and confining, and it is felt that the modeled behavior in car-to-car collisions does not accurately represent the actual phenomena.
- Numerical simulation of the collision between vehicles should be extended to include collision at several degrees of alignment and several levels of engagement. Performance measures should be established that could be used for quantification of crash response and for communicating information between the experimental, semi-empirical and detailed FEM crash-modeling methods.

## ACKNOWLEDGMENTS

The American Iron and Steel Institute (AISI) under Project Number ERD-97-XM001 with the U.S. Department of Energy sponsored the research discussed in this paper. Work was performed at the Oak Ridge National Laboratory (ORNL), which is managed by UT-Battelle, LLC, for the U.S. Department of Energy under contract DE-AC05-00OR22725.

The authors wish to thank the Safety Panel of AISI for their support in writing this paper. In addition to that the authors like to thank Jon Harrington from AISI for reviewing the paper. They also would like to thank the Automotive Applications Committee of AISI as well as management of ORNL for granting the opportunity to submit this paper.

Last, the ULSAB consortium needs to be recognized for granting permission to use the ULSAB study - the project was conducted by Porsche Engineering Services, Inc., and finished in 1998 - as basis for the work done by ORNL.

The American Iron and Steel Institute (AISI) is a non-profit association of North American companies engaged in the iron and steel industry. The Institute comprises 47 member companies, including integrated and electric furnace steelmakers, and 178 associate and affiliate members who are suppliers to or customers of the steel industry. Member companies account for more than two-thirds of the raw steel produced in the U.S., most of the steel manufactured in Canada and nearly two-thirds of the flat-rolled steel products manufactured in Mexico. For a broader look at steel and its applications, the Institute has its own web sites at <http://www.steel.org> and <http://www.autosteel.org>

## CONTACT

For additional information on the details of the research project please contact Srdan Simunovic, [simunovics@ornl.gov](mailto:simunovics@ornl.gov). Srdan Simunovic is a materials research engineer in the Computational Materials Science Group, <http://www-cms.ornl.gov>, at the Oak Ridge National Laboratory. For additional information on the scope and other AISI related areas please contact Marcel van Schaik, [vanschaim@autosteel.org](mailto:vanschaim@autosteel.org). Marcel van Schaik is the manager of the Advanced Materials Technology at the American Iron and Steel Institute.

## REFERENCES

- 1 Jawad, S., Compatibility Analysis of Vehicle-to-Vehicle in Head-on Collision, AMD-Vol. 225/BED-Vol.38, Crashworthiness, Occupant Protection and Biomechanisms in Transportation Systems, ASME 1997.
- 2 Zobel, R., Accident Analysis and Measures to Establish Compatibility, paper 1999-01-0065, Vehicle Aggressivity and Compatibility in Automotive Crashes (SP-1442) SAE, March 1999.
- 3 Gabler, H., and Flides, B., Car Crash Compatibility: The Prospect for International Harmonization, paper 1999-01-006, Vehicle Aggressivity and Compatibility in Automotive Crashes (SP-1442) SAE, March 1999.
- 4 Crash Compatibility Status Report, Insurance Institute for Highway Safety, February 1998.
- 5 Simunovic, S., Aramayo, G., Zacharia, T., Toridis, Bandak, F. and Ragland, C., Advanced Computational Simulation for Design and Manufacturing of Lightweight Material Components for Automotive Applications, ORNL/TM-13407, Oak Ridge, TN, 1997.
- 6 Bedewi, N. E. and Kan, C. D. and Summers, S. Ragland, C., Evaluation of Car-to-Car Frontal Offset Impact Finite Element Models Using Full Scale Crash Data, SAE World Congress, 1995.
- 7 Gupta, V., Gunasekar, T. Rao, A., Kamarajan, J. and Summers, S., Reverse Engineering Method for Developing Passenger Vehicle Finite Element Models, SAE paper 1999-01-0083, International Congress and Exposition, Detroit, Mi., 1999.
- 8 Ultralight Steel Auto Body Final Report, Porsche Engineering Services, Inc. March 1998.
- 9 Hallquist, J., LS-DYNA Keyword User's Manual- Nonlinear Dynamic Analysis of Structures, Version 950, May 1999.
- 10 Communication: Barsan-Anelli, A. (NHTSA) to Aramayo, G., Finite Elements Models of Passenger Cars, May 2000.
- 11 Paluzny, A., State-of-the-Art Review of Automobile Structural Crashworthiness, AISI Publication AU2301 (1051), 1993.
- 12 Agaram, V., Xu, L., Wu, J., Kostyniuk, G., Nusholtz, G., Comparison of Frontal Crash Test Pulses, Automotive Engineering International, July 2000.